

Magnetic and transport properties of the pseudobinary systems $\text{Ce}(\text{Fe}_{1-x}\text{Co}_x)_2$ and $(\text{Ce}_{1-y}\text{Sc}_y)\text{Fe}_2$

H. Fukuda, H. Fujii,* and H. Kamura

Faculty of Integrated Arts & Sciences, Hiroshima University, Higashi-Hiroshima 739-8521, Japan

Y. Hasegawa, T. Ekino, N. Kikugawa, T. Suzuki, and T. Fujita

Graduate School of Advanced Sciences of Matter, Hiroshima University, Higashi-Hiroshima 739-8526, Japan

(Received 3 April 2000; revised manuscript received 10 July 2000; published 3 January 2001)

We studied the dilute substitution effect on magnetic and transport properties in an unstable ferromagnet CeFe_2 with a C15 cubic Laves-phase structure. In the Co substitution system $\text{Ce}(\text{Fe}_{1-x}\text{Co}_x)_2$ with $x \leq 0.10$, while the Curie temperature T_C decreases with increasing the Co concentration, an antiferromagnetic ordering appears in the low temperature region for $x \geq 0.05$, and the transition temperature T_0 from ferromagnetic to antiferromagnetic states monotonously increases with increasing the Co concentration. On the other hand, in the Sc substitution system $(\text{Ce}_{1-y}\text{Sc}_y)\text{Fe}_2$ with $y \leq 0.10$, both the Curie temperature T_C and saturation magnetization M_S at 4.2 K gradually increase with increasing the Sc concentration. Despite the decrease in lattice parameter upon substitution in both the systems, an antiferromagnetic ground state is stabilized in $\text{Ce}(\text{Fe}_{1-x}\text{Co}_x)_2$, whereas a ferromagnetic ground state is stabilized in $(\text{Ce}_{1-y}\text{Sc}_y)\text{Fe}_2$. These results indicate that the Fe 3d–Fe 3d ferromagnetic exchange interaction and the antiferromagnetic spin correlation arising from the Ce 4f–Fe 3d hybridization compete in CeFe_2 , and the enhancement/depression of the 4f–3d hybridization effect might make the ferromagnetic ground state in CeFe_2 unstable/stable. Furthermore, $\text{Ce}(\text{Fe}_{1-x}\text{Co}_x)_2$ exhibited a negative giant magnetoresistance reaching about $\Delta\rho/\rho \sim 60\text{--}65\%$ at 4.2 K, which is accompanied by a metamagnetic transition from antiferromagnetic to ferromagnetic states. The giant magnetoresistance effect is originated from the reconstruction of Fermi surface due to the collapse of the superzone gap after the metamagnetic transition.

DOI: 10.1103/PhysRevB.63.054405

PACS number(s): 75.30.Mb, 75.50.Cc, 75.70.Pa

I. INTRODUCTION

CeFe_2 crystallizes in the MgCu_2 -type cubic C15 Laves phase structure and is an itinerant ferromagnet with the Curie temperature of $T_C = 230$ K and the spontaneous magnetization of $M_S = 2.3 \mu_B/\text{f.u.}$ at 4.2 K.¹ CeFe_2 is quite unique because of the lowest T_C and smallest M_S among the series of the $R\text{Fe}_2$ (R = rare earth metals) system. In addition, it is known that a small amount of substitution of other metals Al, Co, Ru, Ir, Re, and Os for Fe makes the ground state antiferromagnetic,^{2–13} irrespective of changing the lattice spacing upon substitution, while the substitution of Ni, Mn, Rb, and Pd leaves the ground state ferromagnetic like simple dilution.^{3,6,7}

Much attention have been also paid in the character of 4f electron in CeFe_2 , because Eriksson *et al.* predicted the existence of a magnetic moment on the Ce atom, the direction of which is opposite to that on the Fe atoms, and a quenching of the orbital 4f moment.¹⁴ A polarized neutron diffraction study showed that the values of Fe and Ce moments were $\mu_{\text{Fe}} = 1.174 \mu_B$ and $\mu_{\text{Ce}} = -0.14 \mu_B$, respectively.¹⁵ In addition, the magnetic circular x-ray dichroism (MCXD) experiments^{16–19} and magnetic Compton scattering study²⁰ have been carried out for determining the value of an ordered Ce moment, but the deduced values of Ce moments were widely scattered from $-0.57 \mu_B$ to $-0.14 \mu_B$. However, all the values of the Ce moments deduced are oppositely directed to those on the Fe atoms. Furthermore, Giorgetti *et al.* compared the MCXD signals for CeFe_2 with those of $\text{Ce}(\text{Fe}_{0.8}\text{Co}_{0.2})_2$, and concluded that the Co substitution in CeFe_2 did not affect on the Ce magnetic moment.¹⁷ There-

fore, it seems that the strong effect of substitution in $\text{Ce}(\text{Fe}, M)_2$ ($M = \text{Co}, \text{Al}, \text{Ru}$, and so on) on basic magnetism does not come from the change in the magnetic state of the Ce sublattice, but rather come from instabilities of the magnetic structure of the Fe sublattice itself. These results suggest the importance of the hybridization effect between itinerant Ce 4f electron and Fe 3d electron in the static ground state in CeFe_2 .

In 1998, Paolasini *et al.*²¹ have probed the Fe magnetic instability in CeFe_2 by neutron inelastic scattering. They observed a strong antiferromagnetic (AF) spin fluctuation with an energy of ~ 1 meV around the reciprocal lattice point $[1/2, 1/2, 1/2]$ in the Brillouin zone, which corresponds to a static AF component of about $0.05 \mu_B$ in the ferromagnetic ground state. It should be noted that such an unusual AF spin fluctuation does not absolutely exist in UFe_2 , in which the 5f electrons are itinerant.²² Furthermore, the spin-wave stiffness constant D of CeFe_2 is greatly reduced compared to that found in YFe_2 , while the spin-wave stiffness of UFe_2 is enhanced.^{21–23} In addition, UFe_2 has the low Fe magnetic moment and the significantly low Curie temperature T_C compared to those in YFe_2 and CeFe_2 . Therefore, it seems that the U 5f–Fe 3d hybridization results in strong enhancement of the spin-wave stiffness constant D , while the Ce 4f–Fe 3d hybridization effect brings the reduction of the spin-wave stiffness constant D as well as the development of AF spin fluctuations in CeFe_2 . Hence, the AF spin fluctuations in the Fe sublattice seems to be very important in understanding the intrinsic magnetic properties of CeFe_2 .

In this paper, we present the experimental results of the dilutely Co and Sc substitution effects on the magnetic and

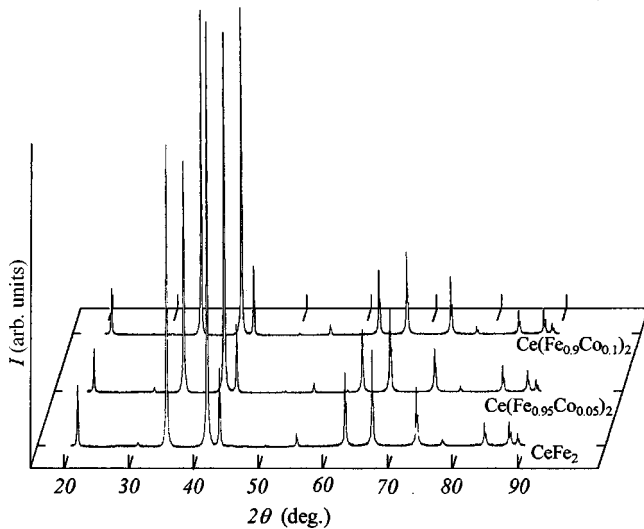


FIG. 1. X-ray diffraction patterns using Cu $K\alpha$ radiation at room temperature for $\text{Ce}(\text{Fe}_{1-x}\text{Co}_x)_2$ with $x=0, 0.05,$ and 0.10 .

transport properties in CeFe_2 performed to gain a deeper insight into the instability of ferromagnetic ground state in CeFe_2 and discuss on the importance of Ce $4f$ -Fe $3d$ hybridization.

II. EXPERIMENT

Polycrystal specimens of CeFe_2 , $\text{Ce}(\text{Fe}_{1-x}\text{Co}_x)_2$ with $x=0.05$ and 0.10 , and $(\text{Ce}_{1-y}\text{Sc}_y)\text{Fe}_2$ with $y=0.03, 0.05,$ and 0.10 were prepared by arc-melting the mixture of stoichiometric amounts of Fe, Co, Sc, and a small amount of excess Ce than the stoichiometry with the purities of 99.99% in Ar flow atmosphere. In order to ensure homogeneity, the ingot was turned over and remelted several times. The ingots were wrapped by Ta foil and then were annealed at 850°C for one week in evacuated quartz tube. All the samples of $\text{Ce}(\text{Fe}_{1-x}\text{Co}_x)_2$ and $(\text{Ce}_{1-y}\text{Sc}_y)\text{Fe}_2$ thus obtained were examined by the powder x-ray diffraction studies at room temperature. As an example, the x-ray diffraction profiles of the Co substitution system are shown in Fig. 1. It is indicative that the samples are almost in a single-phase of the MgCu_2 -type cubic C15 Laves-phase structure with no other extra peaks due to impurity phase, neither α -Fe nor the $\text{Ce}_2\text{Fe}_{17}$ phases except for a very weak Ce oxide peak around $2\theta=30^\circ$.

Magnetization measurement in magnetic fields up to 1.6 T was performed using a vibrating-sample magnetometer (VSM) in temperature ranges from 4.2 to 300 K. High field magnetization measurements up to 5.5 T were done by a superconducting quantum interference device (SQUID) magnetometer in temperature ranges from 5 to 300 K. Electrical resistivity measurements were carried out by a standard DC four-probe technique in magnetic fields up to 9.0 T in temperature ranges from 4.2 to 300 K. Magnetoresistance was measured at 5.0 K in magnetic fields up to 9.0 T, in which the direction of magnetic field was perpendicular to the current direction. The tunneling measurement was performed at 4.2 K using a break-junction method in which the sample

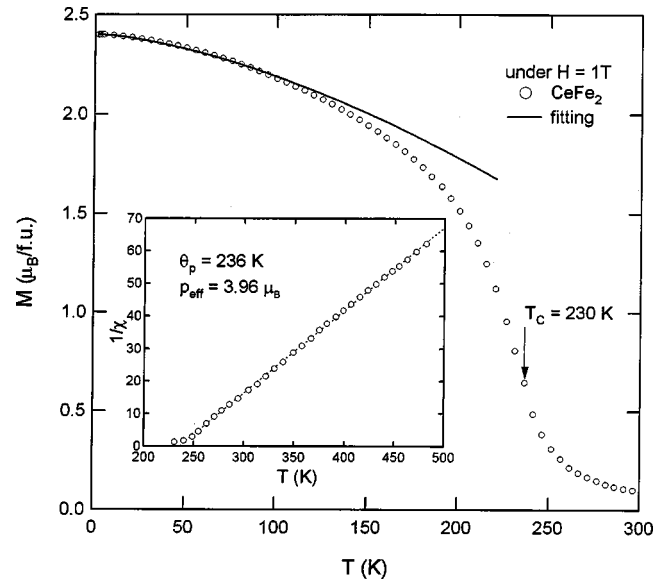


FIG. 2. Temperature dependence of magnetization for CeFe_2 under $H=1.0$ T. The reciprocal susceptibility as a function of temperature above T_C is shown in the inset.

was *in situ* cracked at liquid helium temperature. Generally, fabrication of the artificial tunneling barrier on Ce based compounds has been difficult due to their chemically very reactive surface characteristics. The break-junction method, however, provides a very useful way to investigate this class of materials.^{24,25} The differential conductance dI/dV was directly obtained by a constant ac-modulation technique with a four-probe method.

III. RESULTS AND DISCUSSION

A. Temperature dependence of magnetism in CeFe_2

Figure 2 shows the temperature dependence of magnetization for CeFe_2 under $H=1.0$ T and the inset shows the reciprocal susceptibility as a function of temperature up to 500 K. Here, it was ensured that the magnetic field of 1.0 T was enough to saturate the magnetization by measuring the magnetization vs magnetic field curves at various temperatures. As is evident from Fig. 2, CeFe_2 shows a typical ferromagnetic behavior with the Curie temperature of $T_C=230$ K and the saturation magnetization at 4.2 K of $M_S=2.4 \mu_B/\text{f.u.}$, in spite of the existence of antiferromagnetic spin fluctuations in ferromagnetic ground state.

The temperature dependence of saturation magnetization at low temperatures might be explained by considering the spin wave excitation and the Stoner excitation as follows:

$$M(T)/M(0) = 1 - (\alpha T^{3/2} + \beta T^2), \quad (1)$$

where $M(0)$ is the saturation magnetization at $T=0$ K, and α and β are the parameters indicating the degree of the contributions of the spin wave excitation and the Stoner excitation, respectively. The coefficient of $T^{3/2}$ term, α , and that of T^2 term, β , are deduced to be 8.11×10^{-5} and 7.20×10^{-7} , respectively, by a least square fitting with the experimental data. The calculated result using Eq. (1) is drawn by the solid

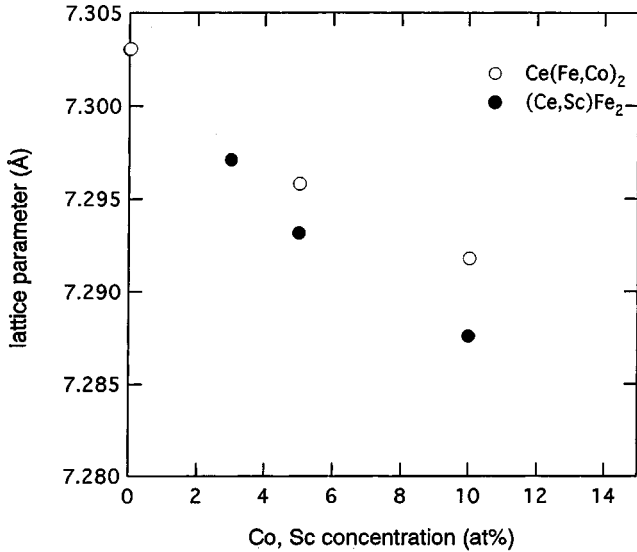


FIG. 3. Lattice parameters of $\text{Ce}(\text{Fe}_{1-x}\text{Co}_x)_2$ and $(\text{Ce}_{1-y}\text{Sc}_y)\text{Fe}_2$ as a function of the substituted Co and Sc concentrations.

line in Fig. 1. The M_s vs T curve at low temperatures is reproduced by the combination of the large component of spin wave excitation and a small component of the Stoner excitation. Here, the coefficient α in $T^{3/2}$ law is connected to a spin-wave stiffness constant D as follows:

$$\alpha = [2.61g\mu_B/M(0)]/(k_B/4\pi D)^{3/2}, \quad (2)$$

where g is the g -factor being equal to 2, μ_B is the Bohr magneton, and k_B is the Boltzmann constant. The spin-wave stiffness constant D could be estimated using Eq. (2) from the coefficient α observed, the value of which was $\sim 130 \text{ meV \AA}^{-2}$. This value is good agreement with $D = 155 \text{ meV \AA}^{-2}$ deduced from a ferromagnetic spin-wave dispersion curve in low q ranges measured by neutron inelastic scattering.²¹ Therefore, we conclude that the temperature dependence of static saturation magnetization in CeFe_2 is understandable by the spin wave excitation and a small contribution of the Stoner excitation, even though the antiferromagnetic spin fluctuations exist in the ferromagnetic ground state. For the Co substitution system, we could not analyze the temperature dependence of saturation magnetization because the magnetic field of 1.0 T is too weak to ferromagnetically saturate the magnetization in antiferromagnetic state at low temperatures.

As is shown in the inset, the inverse susceptibility of CeFe_2 follows a Curie-Weiss law above 270 K with the paramagnetic Curie temperature of $\theta_p = 236 \text{ K}$ and the effective number of Bohr magneton, $p_{\text{eff}} = 3.96 \mu_B$, per Fe atom. This value is comparable to that reported by D eportes *et al.*²⁶ Assuming that Ce is in a nonmagnetic state, the value of magnetic moment, $p_c = gS$, in the paramagnetic state is estimated to be $3.08 \mu_B$ per Fe atom. Hence, the ratio of p_c to saturation moment p_s at 0 K, $p_c/p_s = 2.6$, considerably deviates from one, indicating that CeFe_2 is characterized as a typical itinerant ferromagnet.

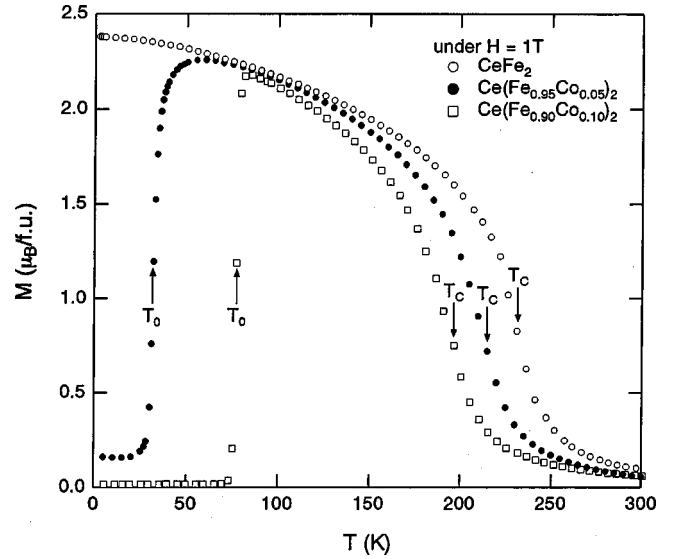


FIG. 4. Temperature dependence of the magnetization for $\text{Ce}(\text{Fe}_{1-x}\text{Co}_x)_2$ under $H = 1 \text{ T}$.

B. Substitution effect on magnetism in CeFe_2

Figure 3 shows the lattice parameters a determined by the powder x-ray diffraction pattern as a function of the Co or Sc concentration. As is evident from Fig. 3, the lattice parameter monotonously decreases with increasing the substitution concentration in both the systems, indicating that a negative chemical pressure acts in CeFe_2 by both the substitutions.

1. The Co substituted system $\text{Ce}(\text{Fe}_{1-x}\text{Co}_x)_2$

Figure 4 shows the temperature dependence of magnetization under $H = 1.0 \text{ T}$ for the dilutely Co substituted system $\text{Ce}(\text{Fe}_{1-x}\text{Co}_x)_2$. In the range of $x \leq 0.10$, the Curie temperature T_C monotonously decreases with increasing the Co concentration. In addition, an antiferromagnetic-like ordering appears for $x = 0.05$ below 30 K and the characteristic temperature of the ferromagnetic-antiferromagnetic transition T_0 increases with increasing the Co concentration. The behavior observed in $\text{Ce}(\text{Fe}_{1-x}\text{Co}_x)_2$ is consistent with the magnetic phase diagram deduced by Rastogi and Murani,³ and Kennedy *et al.*²⁷ In this paper, we focus on only the magnetic properties in dilutely Co substituted regime, in which an antiferromagnetic correlation develops even in ferromagnetic ground state. As is seen in Fig. 4, we notice that a small ferromagnetic component appears at low temperatures in the M vs T curve for $x = 0.05$. In this work, we tried to make the $\text{Ce}(\text{Fe}_{0.95}\text{Co}_{0.05})_2$ samples for two times by the same method as used here and once by the different annealing process proposed by Roy and Coles.⁶ However, the results obtained were almost the same as described above for all three samples. Therefore, we believe that it is intrinsic that a small ferromagnetic component exists at low temperatures in the system with $x = 0.05$, suggesting the appearance of a canted spin structure in which antiferromagnetic and ferromagnetic spin components coexist at $H = 1 \text{ T}$. Similarly, it has been confirmed that a canted spin phase existed below 60 K in

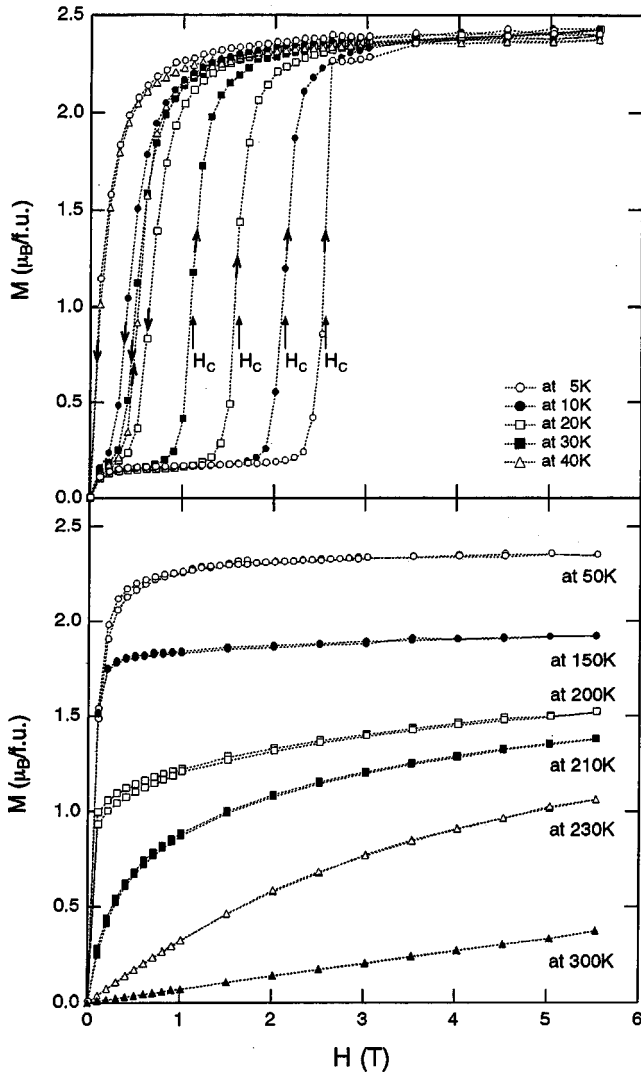


FIG. 5. Isothermal magnetization curves for $\text{Ce}(\text{Fe}_{0.95}\text{Co}_{0.05})_2$ at various temperatures.

$\text{Ce}(\text{Fe}_{0.98}\text{Ru}_{0.02})_2$ by neutron diffraction experiments,¹⁰ which shows similar static magnetic properties to those obtained in $\text{Ce}(\text{Fe}_{0.95}\text{Co}_{0.05})_2$.

Figure 5 shows the isothermal magnetization curve for $\text{Ce}(\text{Fe}_{0.95}\text{Co}_{0.05})_2$ at various temperatures. At 5 K the M vs H curve of $\text{Ce}(\text{Fe}_{0.95}\text{Co}_{0.05})_2$ shows a small ferromagnetic component at low magnetic fields in magnetic field increasing process. With further increasing the magnetic field, a metamagnetic transition occurs at $H_c = 2.5$ T, leading to an induced ferromagnetic state. The metamagnetic transition field H_c is irreversible and accompanied with a large hysteresis. Therefore, in magnetic field decreasing process, the step of magnetization corresponding to the canted magnetic phase with a small ferromagnetic component could not be observed at low magnetic fields, only leaving a small remanent magnetization at $H = 0$. On the other hand, the magnetoresistance effect, which will be described later, indicates that the field-induced ferromagnetism in $\text{Ce}(\text{Fe}_{0.95}\text{Co}_{0.05})_2$ is frozen at 5 K at demagnetized state (see Fig. 9). Therefore, we conclude that $\text{Ce}(\text{Fe}_{0.95}\text{Co}_{0.05})_2$ at 5 K is in a canted spin structure with

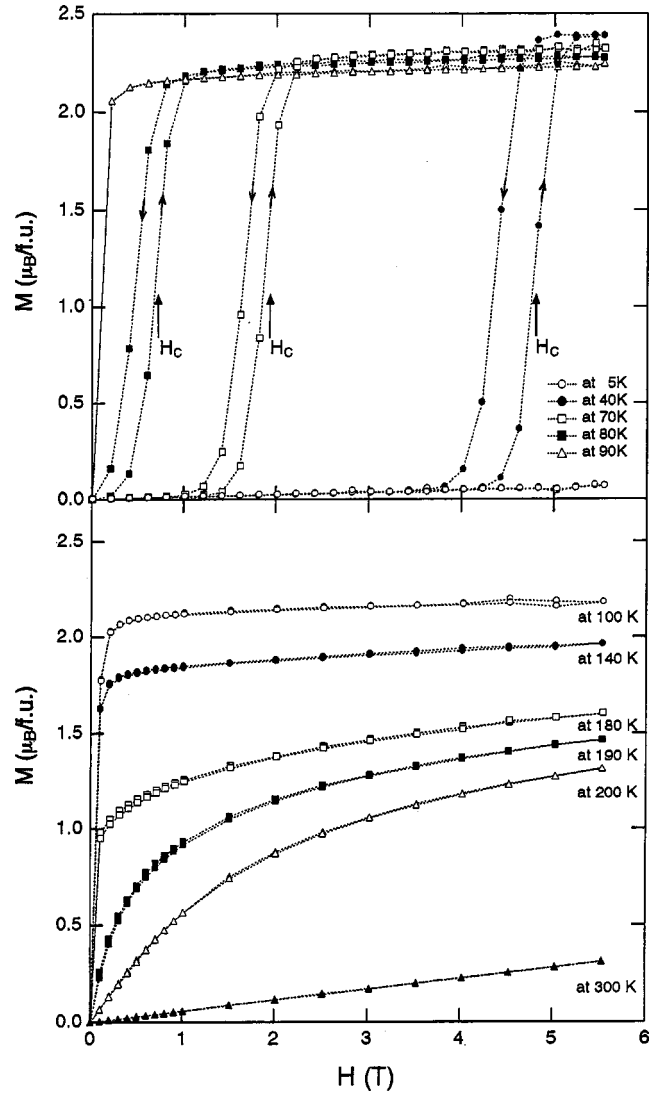


FIG. 6. Isothermal magnetization curves for $\text{Ce}(\text{Fe}_{0.90}\text{Co}_{0.10})_2$ at various temperatures.

ferromagnetic and antiferromagnetic spin components in zero magnetic field, and the ferromagnetism is field-induced with increasing in magnetic field after the first order metamagnetic transition at $H_c = 2.5$ T, which is frozen at 5 K. With increasing temperature, the metamagnetic transition field H_c shifts to lower magnetic field and the canted spin structure becomes stable even in magnetic field decreasing process, accompanied by decreasing the hysteresis of H_c . Above 50 K, the M vs H curve shows a typical ferromagnetic behavior as shown in Fig. 5.

With further increasing the Co concentration, the magnetization for $\text{Ce}(\text{Fe}_{0.90}\text{Co}_{0.10})_2$ at 5 K slightly increases with increasing magnetic field up to 5.5 T as shown in Fig. 6. This indicates that the canted spin state with a ferromagnetic component is not induced in $\text{Ce}(\text{Fe}_{0.90}\text{Co}_{0.10})_2$ at 5 K, which is in a complete antiferromagnetic ordering at least up to 5.5 T. At 40 K, the metamagnetic transition is observed at $H_c = 4.7$ T, the field of which decreases with further increasing temperature and finally disappears above 90 K. In the temperature range from 90 to 190 K, a typical ferromagnetic

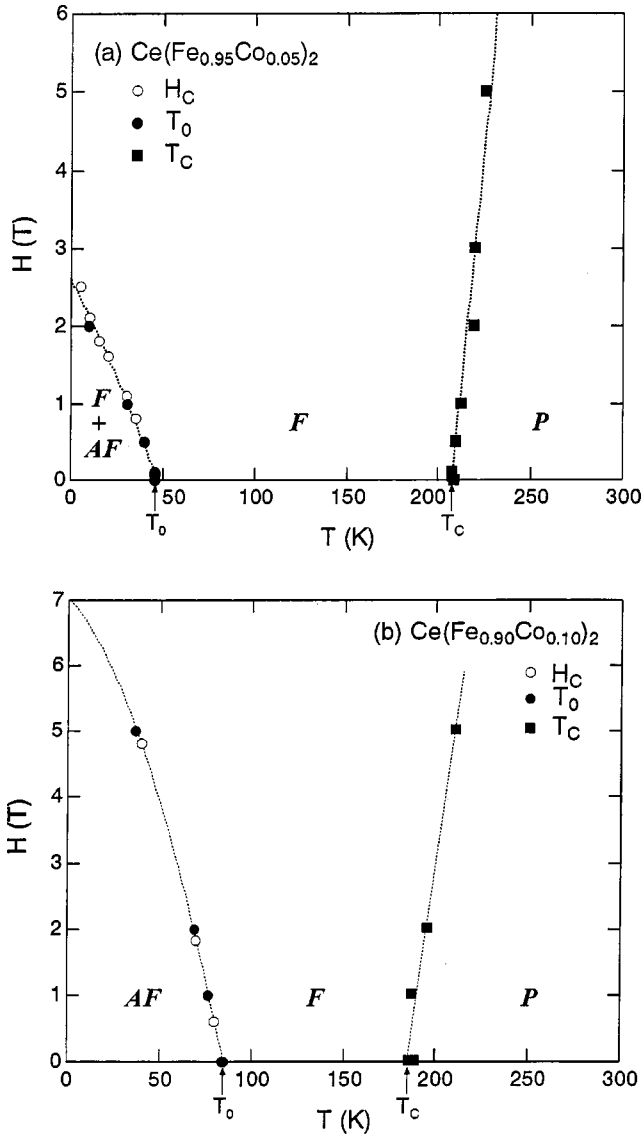


FIG. 7. H - T magnetic phase diagrams for (a) $\text{Ce}(\text{Fe}_{0.95}\text{Co}_{0.05})_2$ and (b) $\text{Ce}(\text{Fe}_{0.90}\text{Co}_{0.10})_2$.

behavior in the M vs H curve is observable as well.

The H - T magnetic phase diagrams deduced from magnetization measurements are shown in Figs. 7(a) and 7(b) for $\text{Ce}(\text{Fe}_{1-x}\text{Co}_x)_2$ with $x=0.05$ and 0.10 , respectively. For the case of $\text{Ce}(\text{Fe}_{0.95}\text{Co}_{0.05})_2$ in Fig. 7(a), it is to be noted that the canted spin phase appears in low magnetic field region at low temperatures. This canted spin state may be induced as a result of the competition between the antiferromagnetic correlation arising from $\text{Ce } 4f$ - $\text{Fe } 3d$ hybridization and the $\text{Fe } 3d$ - $\text{Fe } 3d$ ferromagnetic exchange interaction. On the other hand, $\text{Ce}(\text{Fe}_{0.90}\text{Co}_{0.10})_2$ shows a complete antiferromagnetic ordering below 90 K. From the above experimental results, we conclude that the antiferromagnetic phase becomes stable with increasing the Co concentration for $\text{Ce}(\text{Fe}_{1-x}\text{Co}_x)_2$ with $x \leq 0.10$.

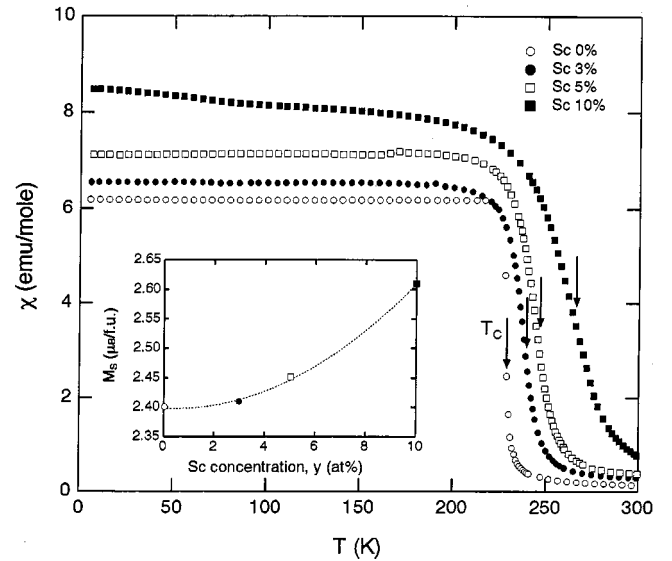


FIG. 8. Temperature dependence of the magnetic permeability at $H=0.1$ T for $(\text{Ce}_{1-y}\text{Sc}_y)\text{Fe}_2$. The inset shows a saturation magnetization at 4.2 K as a function of the substituted Sc concentration.

2. The Sc substituted system $(\text{Ce}_{1-y}\text{Sc}_y)\text{Fe}_2$

Figure 8 shows the temperature dependence of the permeability at $H=0.1$ T for $(\text{Ce}_{1-y}\text{Sc}_y)\text{Fe}_2$ with $y \leq 0.10$. In the inset are shown the saturation magnetization at 4.2 K as a function of the Sc concentration. With increasing the Sc concentration, the Curie temperature rises from $T_C=230$ K for CeFe_2 to $T_C=270$ K for $(\text{Ce}_{0.90}\text{Sc}_{0.10})\text{Fe}_2$. In addition, the saturation magnetization at 4.2 K monotonously increases with increasing the Sc concentration. These results indicate that the Sc substitution for Ce in CeFe_2 makes ferromagnetic ground state stable, even though the lattice parameter decreases with increasing the Sc content. This behavior is clearly in contrast to the result in the dilutely Co substituted system as well as the decrease in T_C under the hydrostatic pressure in CeFe_2 .²⁸ On the other hand, it has been reported that T_C for YFe_2 , GdFe_2 , HoFe_2 , and ErFe_2 linearly increased with increasing pressure.²⁸ The increase in T_C , which is a common feature of $R\text{Fe}_2$ with stable $4f$ electrons and no $4f$ electron, suggests that the $\text{Fe } 3d$ - $\text{Fe } 3d$ ferromagnetic exchange interaction strengthens by the contraction of the lattice even in CeFe_2 similarly to the other $R\text{Fe}_2$ system.

C. Discussion on the magnetism in substitution systems

Despite the contraction of the lattice upon substitution in both the Co and Sc systems, an antiferromagnetic ground state is stabilized in the Co diluted $\text{Ce}(\text{Fe}_{1-x}\text{Co}_x)_2$ system, whereas a ferromagnetic ground state is stabilized in the Sc diluted $(\text{Ce}_{1-y}\text{Sc}_y)\text{Fe}_2$ system. We interpret this contrast behavior under the following three assumptions. (1) In CeFe_2 , there is a competition between the $\text{Fe } 3d$ - $\text{Fe } 3d$ ferromag-

netic exchange interaction and the antiferromagnetic spin correlation due to Ce $4f$ -Fe $3d$ hybridizations. (2) The enhancement of the Ce $4f$ -Fe $3d$ hybridizations strongly suppresses the Curie temperature T_C and the saturation magnetization M_S . (3) The Fe $3d$ -Fe $3d$ ferromagnetic exchange interaction strengthens by the constriction of the lattice even in CeFe₂, similarly to the other RFe₂ system.

On the basis of the above assumptions, (1) in the dilutely Sc substituted system (Ce_{1-y}Sc_y)Fe₂, the ferromagnetism is stabilized by the suppression of the Ce $4f$ -Fe $3d$ hybridizations due to the decrease of the Ce concentration in addition to the enhancement of the Fe $3d$ -Fe $3d$ ferromagnetic exchange interaction due to the constriction of the lattice. On the other hand, (2) the monotonous decrease in Curie temperature T_C under high pressures in CeFe₂ can be explained by the idea that the enhancement of the antiferromagnetic spin correlation through the strengthening of Ce $4f$ -Fe $3d$ hybridizations under pressure exceeds to the strengthening of the Fe $3d$ -Fe $3d$ ferromagnetic exchange interaction due to the contraction of lattice. If there is no hybridization in this system, T_C should increase under high pressures like in the other RFe₂ systems. In the Co diluted system Ce(Fe_{1-x}Co_x)₂, (3) since the lattice parameter decreases with increasing the Co concentration, the Fe $3d$ -Fe $3d$ ferromagnetic exchange interaction is strengthened and the Ce $4f$ -Fe $3d$ hybridizations are simultaneously enhanced. As a result of the fact that the enhancement of antiferromagnetic correlation due to the hybridizations exceeds to the strengthening of ferromagnetic exchange interaction by substituting Co for Fe, the Curie temperature T_C decreases with increasing Co content and the antiferromagnetism is stabilized as well. Similarly, this scenario may explain that all the substitutions of Al, Ru, Ir, Re, and Os for Fe site induce an antiferromagnetic ordering at low temperatures, irrespective of changing the lattice spacing.²⁻¹³ (4) To stabilize the static antiferromagnetism, it is needed that the dynamical antiferromagnetic spin fluctuation in the ferromagnetic state is trapped on the substituting atomic sites at low temperatures, even if the the Ce $4f$ -Fe $3d$ hybridizations is enhanced by substitution. This idea is consistent with the results of recent inelastic neutron scattering studies performed by Paolasini *et al.*,²⁹ in which the antiferromagnetic spin fluctuation still exists around the L points in the Brillouin zone in the ferromagnetic state for Ce(Fe_{0.93}Co_{0.07})₂, but it changes into a typical antiferromagnetic spin wave dispersion with a propagating vector $\tau=[1/2,1/2,1/2]$ in the antiferromagnetic state at low temperatures. Hence, we conclude that the development of the antiferromagnetic spin correlation due to the Ce $4f$ -Fe $3d$ hybridizations makes the ferromagnetic ground state in CeFe₂ unstable upon dilute substitution.

On the other hand, it is known that the substitutions of Ni, Mn, Rh, Pd for Fe in CeFe₂ leads to simple dilution of ferromagnetism. In the above argument, we cannot understand the simple dilution behavior of ferromagnetism, suggesting that we have to take into account the change in electronic band structure upon substitution. The band effect may be also essential for the appearance of antiferromagnetism at low temperatures as well as the volume effect. The change in band structure upon substitution affected on the

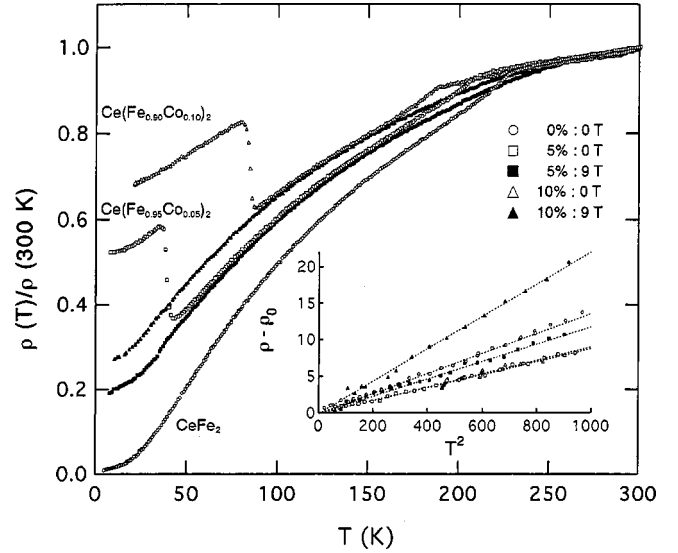


FIG. 9. Temperature dependence of the normalized electrical resistivity $\rho(T)/\rho(300\text{ K})$ for Ce(Fe_{1-x}Co_x)₂ in $H=0$ and 9 T . The inset shows a quadratic temperature dependence of the electrical resistivity.

Ce $4f$ -Fe $3d$ hybridizations and the ferromagnetic Fe $3d$ - $3d$ exchange interaction may be completely different in the two cases of the Al, Co, Ru, Ir, Re, Os substitution and the Mn, Ni, Rh, Pd substitution for Fe in CeFe₂. If both the ferromagnetic Fe $3d$ - $3d$ exchange interaction and the Ce $4f$ -Fe $3d$ hybridizations are suppressed due to the band effect upon the later substitution and the degree of the suppression of the Ce $4f$ -Fe $3d$ hybridizations are much larger than that of ferromagnetic Fe $3d$ - $3d$ exchange interaction, it seems that the Curie temperature T_C gradually decreases upon substitution without appearance of static antiferromagnetism, leading to simple dilution of ferromagnetism. Further studies are needed to clarify the origin of the above unusual substitution behavior.

D. Transport properties in the Co substituting system

Figure 9 shows the temperature dependence of electrical resistivity ρ for the Co substituted system Ce(Fe_{1-x}Co_x)₂, where all the electrical resistivities are normalized by the values at 300 K. The electrical resistivity ρ for both Ce(Fe_{0.95}Co_{0.05})₂ and Ce(Fe_{0.90}Co_{0.10})₂ shows a kink at T_C and a discontinuous increases at the transition temperature T_0 from ferromagnetic to antiferromagnetic states with decreasing temperature. The anomalous increase of ρ in the antiferromagnetic state for both the systems is suppressed by a magnetic field of $H=9\text{ T}$. We have also investigated the isothermal magnetic field effect on ρ . The magnetoresistance $\Delta\rho/\rho=[\rho(H)-\rho(0)]/\rho(0)$ at 5 K is plotted as a function of the magnetic field H in Fig. 10, together with the M vs H curves. For the Co 5% substituting system, a rapid decrease of $\Delta\rho/\rho$ occurs at the metamagnetic transition field of $H_C=2.5\text{ T}$, reaching a negative giant magnetoresistance (GMR) of 64%. Since the magnetization is irreversible, the magne-

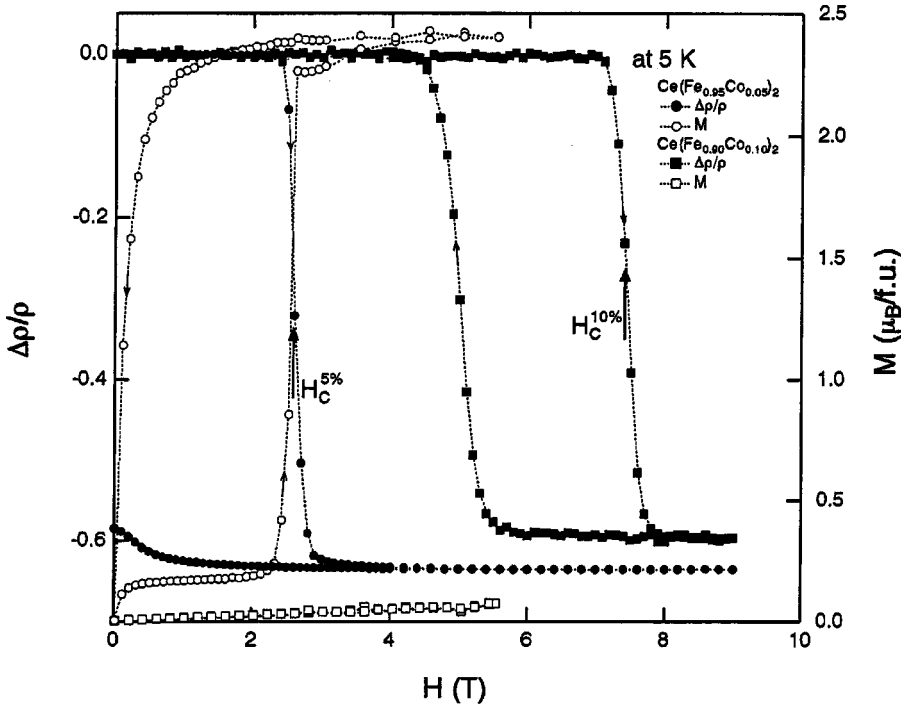


FIG. 10. Magnetoresistance at 4.2 K as a function of the magnetic field, together with the magnetization curves.

toresistance $\Delta\rho/\rho$ does not recover to the initial value, leaving almost the final value at demagnetized state. This indicates that the magnetic state after removing magnetic field is still ferromagnetic, where the ferromagnetism above H_0 is frozen at 5 K. In $\text{Ce}(\text{Fe}_{0.90}\text{Co}_{0.10})_2$, the magnetoresistance $\Delta\rho/\rho$ rapidly decreases at $H_C = 7.5$ T with a hysteresis of about 2 T, reaching a negative GMR of 60% as well. A similar negative GMR was also observed in the Al (Ref. 30) and Ru- (Ref. 31) substitution systems, but the GMR in the Al- and Ru-substitution systems was somewhat smaller. As is shown in the inset of Fig. 9, the electrical resistivity shows a quadratic temperature dependence, i.e., $\rho = \rho_0 + AT^2$ at low temperatures. We notice that in $\text{Ce}(\text{Fe}_{1-x}\text{Co}_x)_2$, the quadratic temperature coefficient in the ferromagnetic state A_F is considerably larger than that in the antiferromagnetic state

A_{AF} . On the basis of Fermi liquid theory, the quadratic temperature coefficient in electrical resistivity A is proportional to the square of the density of states at Fermi level $D^2(\varepsilon_F)$. Hence, it seems that the density of states at Fermi level in the ferromagnetic state is larger than that in the antiferromagnetic state, $D(\varepsilon_F)_F > D(\varepsilon_F)_{AF}$. This is consistent with the behavior of the electronic specific heat coefficient γ , that is $\gamma_F > \gamma_{AF}$ deduced by Wada *et al.*³² These results simply suggest that the gaplike feature is formed near the Fermi level in the antiferromagnetic state, leading to decrease in the density of state at ε_F due to small Fermi surface, and the density of states at ε_F increases when ferromagnetism is recovered by the metamagnetic transition. To clarify the formation of the gaplike feature, we measured the tunneling spectra in this work.

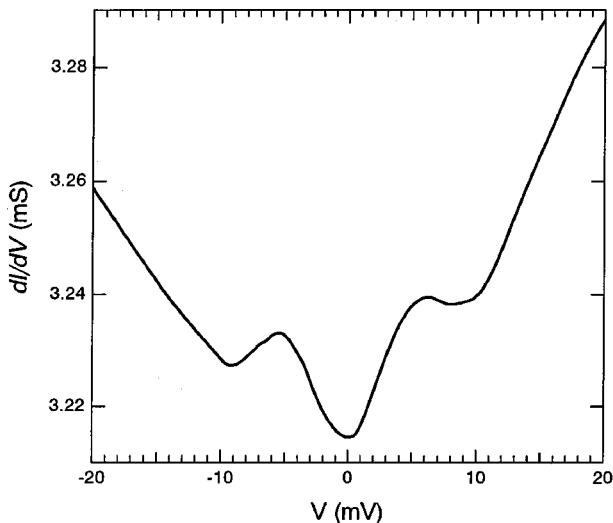


FIG. 11. Tunneling conductance for $\text{Ce}(\text{Fe}_{0.95}\text{Co}_{0.05})_2$ at 4.2 K.

Figure 11 shows the tunneling spectra of $\text{Ce}(\text{Fe}_{0.95}\text{Co}_{0.05})_2$ at 4.2 K in zero magnetic field.³³ The result obtained clearly indicates the existence of a gap structure with the width of $2\Delta = \sim 10$ meV on the V-shape background near the zero-bias voltage which corresponds to the Fermi level. A similar gap structure was also observed in $\text{Ce}(\text{Fe}_{0.90}\text{Co}_{0.10})_2$ with $2\Delta = 19$ meV, the value of which is almost twice of that in $\text{Ce}(\text{Fe}_{0.95}\text{Co}_{0.05})_2$. We notice that the gap width is proportional to the transition temperature T_0 from ferromagnetic to antiferromagnetic states. This suggests, in the system $\text{Ce}(\text{Fe}_{1-x}\text{Co}_x)_2$ with $x = 0.05$ and 0.10 , that a superzone gap opens near the Fermi level in the antiferromagnetic state. Therefore, we can understand the appearance of negative GMR in the Co substituted system $\text{Ce}(\text{Fe}_{1-x}\text{Co}_x)_2$ by the following scenario. (1) With decreasing the temperature, the superzone gap is formed near the Fermi level below the ferromagnetic-antiferromagnetic transition temperature T_0 and as a result of gap formation, the electrical resistivity suddenly increases. (2) However, the electrical resistivity does not follow a thermal activation type behavior because

of the formation of the anisotropic gap, reflecting the direction of a propagation vector in an antiferromagnetic structure. (3) At low temperatures, since the superzone gap is collapsed with the metamagnetic transition from antiferromagnetic to ferromagnetic state, the Fermi surface is reconstructed and the cross section of the Fermi surface becomes large. (4) Finally, as a result of recovery of the carrier numbers, the negative GMR occurs.

IV. SUMMARY

In order to gain a deeper insight to instability of ferromagnetic ground state in CeFe_2 , we studied the dilute Co and Sc substitution effects on the magnetic and transport properties. In the Co substituted system $\text{Ce}(\text{Fe}_{1-x}\text{Co}_x)_2$ for $x \leq 0.10$, while the Curie temperature T_C decreases with increasing the Co concentration, an antiferromagnetic ordering appears for $x \geq 0.05$ at low temperatures and the transition temperature T_0 from ferromagnetic to antiferromagnetic states monotonously increases with increasing x , leading to an instability of the ferromagnetism in CeFe_2 . On the other hand, in the Sc substituted system $(\text{Ce}_{1-y}\text{Sc}_y)\text{Fe}_2$, both the Curie temperature T_C and the saturation magnetization M_S at 4.2 K increase with increasing the Sc concentration, indicating the stability of ferromagnetism in CeFe_2 . Despite the constriction of the lattice spacing upon substitution in both the systems, the substitution effect of Sc for Ce on magnetic properties is clearly in contrast to that in the Co substitution system. In $(\text{Ce}_{1-y}\text{Sc}_y)\text{Fe}_2$, the suppression of the antiferromagnetic spin fluctuations due to the decrease of the Ce concentration as well as the enhancement of the ferromagnetic exchange interaction between Fe $3d$ -Fe $3d$ spins due to the lattice constriction makes ferromagnetic ground state stable. On the other hand, the Curie temperature T_C in $\text{Ce}(\text{Fe}_{1-x}\text{Co}_x)_2$ decreases with increasing the Co content because the enhancement of antiferromagnetic spin correlation due to the constriction of lattice exceeds to the increase in strength of Fe $3d$ -Fe $3d$ ferromagnetic exchange interaction. Furthermore, as a result of trapping a dynamical antiferromagnetic spin fluctuations on the substituting Co sites, a long-range antiferromagnetic ordering like a spin density wave SDW develops at low temperatures in $\text{Ce}(\text{Fe}_{1-x}\text{Co}_x)_2$.

The similar features could be realized in the Al, Ru, Ir, Re, and Os substitution systems. However, the contrast behavior in the Ni, Mn, Rh, and Pd substituted systems for Fe in CeFe_2 as simple dilution of ferromagnetism is still unresolved at present. Nevertheless, we can conclude that the Curie temperature T_C and saturation magnetization M_S of CeFe_2 is strongly suppressed by the development of antiferromagnetic spin correlation due to the Ce $4f$ -Fe $3d$ hybridizations in comparison with those of other $R\text{Fe}_2$.

$\text{Ce}(\text{Fe}_{1-x}\text{Co}_x)_2$ with $x=0.05$ and 0.10 show a negative giant magnetoresistance effect reaching $\Delta\rho/\rho=64\%$ and 60% at 4.2 K, respectively. The quadratic temperature coefficient A of electrical resistivity and the electronic specific heat coefficient γ (Ref. 28) in the field induced ferromagnetic state is larger than those in the antiferromagnetic state. Furthermore, the tunneling spectra directly show a gap structure, in which the energy gap 2Δ is proportional to the ferromagnetic-antiferromagnetic transition temperature T_0 . Hence, we concluded that GMR in $\text{Ce}(\text{Fe}_{1-x}\text{Co}_x)_2$ is originated from the increase of carrier numbers due to the collapse of the superzone gap after the metamagnetic transition.

In this paper, it was clarified that the Ce $4f$ -Fe $3d$ hybridizations were important to understand the intrinsic magnetism in CeFe_2 , which might give rise to the AF spin fluctuations of the Fe spins even in a ferromagnetic ground state from the investigation of the Co and Sc substitution effects on magnetic and transport properties. Thus, it is considerably interesting to know how the ferromagnetism in CeFe_2 does change when we apply hydrostatic pressure and the Ce $4f$ -Fe $3d$ hybridizations are enhanced. Magnetization measurements under the hydrostatic pressure using a CeFe_2 single crystal are now in progress, which will be published in elsewhere.

ACKNOWLEDGMENTS

We thank L. Paolasini for useful discussions on the spin fluctuations in CeFe_2 as well as in $\text{Ce}(\text{Fe},\text{Co})_2$. We also thank the cryogenic center in Hiroshima University for supplying liquid helium and for the use of a vibrating sample magnetometer (VSM) to perform magnetization measurements.

*Corresponding author. FAX: (+81)824-24-0757. Email address: hfujii@hiroshima-u.ac.jp

¹J. J. M. Franse and R. J. Radwanski, in *Handbook of Magnetic Materials*, edited by K. H. J. Buschow (Elsevier, Amsterdam, 1993), Vol. 7, p. 207.

²D. F. Franceschini and S. F. D. Cunha, *J. Magn. Magn. Mater.* **52**, 280 (1985).

³A. K. Rastogi and A. P. Murani, in *Theoretical and Experimental Aspects of Valence Fluctuations and Heavy Fermions*, edited by L. C. Gupta and S. K. Malik (Plenum, New York, 1987), p. 437.

⁴S. B. Roy and B. R. Coles, *J. Phys. F: Met. Phys.* **17**, L215 (1987).

⁵S. B. Roy and B. R. Coles, *J. Appl. Phys.* **63**, 4094 (1988).

⁶S. B. Roy and B. R. Coles, *Phys. Rev. B* **39**, 9360 (1989).

⁷A. K. Rastogi, G. Hilscher, E. Gratz, and N. Pillmayr, *J. Phys. Colloq.* **C8**, 277 (1988).

⁸S. B. Roy, S. J. Kennedy, and B. R. Coles, *J. Phys. Colloq.* **C8**, 271 (1988).

⁹S. J. Kennedy, A. P. Murani, J. K. Cockcroft, S. B. Roy, and B. R. Coles, *J. Phys.: Condens. Matter* **1**, 629 (1989).

¹⁰S. J. Kennedy and B. R. Coles, *J. Phys.: Condens. Matter* **2**, 1213 (1990).

¹¹N. Ali and X. Zhang, *J. Phys.: Condens. Matter* **4**, L351 (1992).

¹²G. E. Femandes, M. G. Berisso, O. Trovarelli, and J. G. Sereni, *J. Alloys Compd.* **261**, 26 (1997).

¹³A. K. Rajarajan, S. B. Roy, and P. Chaddah, *Phys. Rev. B* **56**, 7808 (1997).

¹⁴S. J. Kennedy, P. J. Brown, and B. R. Coles, *J. Phys.: Condens.*

- Matter **5**, 5169 (1993).
- ¹⁵O. Eriksson, L. Nordstrom, M. S. S. Brooks, and B. Johansson, Phys. Rev. Lett. **60**, 2523 (1988).
- ¹⁶F. Baudelet, C. Brouder, E. Dartyge, A. Fontaine, J. P. Kappler, and G. Krill, Europhys. Lett. **13**, 751 (1990).
- ¹⁷C. Giorgetti, S. Pizzini, E. Dartyge, A. Fontaine, F. Baudelet, C. Brouder, Ph. Bauer, G. Krill, S. Miraglia, D. Fruchart, and J. P. Kappler, Phys. Rev. B **48**, 12 732 (1993).
- ¹⁸J. Ph. Schill, E. F. Bertran, M. Finazzi, Ch. Brouder, J. P. Kappler, and G. Krill, Phys. Rev. B **50**, 2985 (1994).
- ¹⁹A. Delobbe, A. M. Dias, M. Finazzi, L. Stichauer, J. P. Kappler, and G. Krill, Europhys. Lett. **43**, 320 (1998).
- ²⁰M. J. Copper, P. K. Lawson, M. A. G. Dixon, E. Zukowski, D. N. Timms, F. Itoh, H. Sakurai, H. Kawata, Y. Tanaka, and M. Ito, Phys. Rev. B **54**, 4068 (1996).
- ²¹L. Paolasini, P. Dervenagas, P. Vulliet, J. P. Sanchez, G. H. Lander, A. Hiess, A. Panchula, and P. Canfield, Phys. Rev. B **58**, 12 117 (1998).
- ²²L. Paolasini, G. H. Lander, S. M. Shapiro, R. Caciuffo, B. Lebech, L.-P. Regnault, B. Roessli, and J.-M. Fournier, Phys. Rev. B **54**, 7222 (1996).
- ²³L. Paolasini, R. Caciuffo, B. Roessli, G. H. Lander, K. Myers, and P. Canfield, Phys. Rev. B **59**, 6867 (1999).
- ²⁴T. Ekino, T. Takabatake, H. Tanaka, and H. Fujii, Phys. Rev. Lett. **75**, 4262 (1995).
- ²⁵T. Ekino, H. Fujii, T. Nakama, and K. Yagasaki, Phys. Rev. B **56**, 7851 (1997).
- ²⁶J. Dèportes, D. Givord, and K. R. A. Zeibeck, J. Appl. Phys. **52**, 2074 (1981).
- ²⁷S. J. Kennedy, A. P. Murani, B. R. Coles, and O. Moze, J. Phys. F: Met. Phys. **18**, 2499 (1988).
- ²⁸M. Brouha and K. H. J. Buschow, J. Appl. Phys. **44**, 1813 (1973).
- ²⁹L. Paolasini and G. H. Lander (private communication).
- ³⁰A. K. Nigam, S. Radha, S. B. Roy, and G. Chandra, Physica B **205**, 421 (1995).
- ³¹H. P. Kunkel, X. Z. Zhou, P. A. Stampe, J. A. Cowen, and G. Williams, Phys. Rev. B **53**, 15 099 (1996).
- ³²H. Wada, T. Harada, and M. Shiga, J. Phys.: Condens. Matter **9**, 9347 (1997).
- ³³T. Ekino, Y. Hasegawa, H. Fukuda, H. Kamura, and H. Fujii, Physica B **284–288**, 1327 (2000).